AGU PUBLICATIONS

Geophysical Research Letters

RESEARCH LETTER
10.1002/2015GL067574

Key Point:
- Projected intensification of subseasonal TAS variability

Supporting Information:
- Supporting Information S1

Correspondence to:
H. Teng,
hteng@ucar.edu

Citation:
Teng, H., G. Branstator, G. A. Meehl, and W. M. Washington (2016), Projected intensification of subseasonal temperature variability and heat waves in the Great Plains, *Geophys. Res. Lett., 43*, 2165–2173, doi:10.1002/2015GL067574.

Received 28 DEC 2015
Accepted 29 JAN 2016
Accepted article online 4 FEB 2016
Published online 9 MAR 2016

Projected intensification of subseasonal temperature variability and heat waves in the Great Plains

Haiyan Teng[1], Grant Branstator[1], Gerald A. Meehl[1], and Warren M. Washington[1]

[1]National Center for Atmospheric Research, Boulder, Colorado, USA

Abstract Compared to changes in the climatological mean temperature, we have less confidence in how much and by what mechanisms temperature variability may be affected by anthropogenic climate change. Here based on a 30-member climate change projection from an earth system model, we find that summertime subseasonal temperature variability in the U.S. Great Plains is enhanced by approximately 20% in 2070–2100 relative to 1980–2010. In particular, daily temperature departures from the new climatologies during future heat waves are on average 0.6°C warmer than are the corresponding departures under present-day conditions. Although in both periods heat waves in the Great Plains tend to be associated with planetary wave events, the amplification of future heat waves does not appear to be induced by changes in planetary wave variability in the midlatitudes. Instead, in this experiment the strengthening appears to be primarily caused by enhanced local land-atmosphere feedbacks resulting from a warmer/drier future climate.

1. Introduction

The Northern Hemisphere midlatitudes have been hit by a series of record-breaking heat waves in recent decades, leading to catastrophic socioeconomic impacts and growing public concern about climate change. While more intense and more frequent heat waves are an expected consequence of the rising climatological mean temperature produced by increasing greenhouse gas concentrations [*Meehl and Tebaldi*, 2004], it is still poorly understood to what extent global warming can also affect these extreme events by changing temperature variability [*Katz and Brown*, 1992; *Gregory and Mitchell*, 1995; *Kjellström et al*., 2007; *Fischer et al*., 2011; *Kim et al*., 2013; *Cattiaux et al*., 2015].

Climate models that participated in phase 5 of the Coupled Model Intercomparison Project (CMIP5 [*Taylor et al*., 2012]) tend to project reduced wintertime synoptic temperature variability in midlatitudes in the future warmer climate [*Schneider et al*., 2014; *Screen*, 2014; *Screen et al*., 2015]. However, those models do not yield a robust change regarding the summertime synoptic temperature variability, especially over land [*Schneider et al*., 2014; *Screen*, 2014]. Subseasonal variability can potentially have a strong impact on prolonged and therefore more severe heat waves. Two mechanisms have been proposed by which climate change in the mean state can in turn affect summertime subseasonal temperature variability. One involves local land-atmosphere feedback, the strength of which is sensitive to the mean soil moisture [*Schär et al*., 2004; *Koster et al*., 2004; *Seneviratne et al*., 2006, 2010; *Fischer et al*., 2007, 2012]. The second mechanism involves changes in atmospheric circulation characteristics, possibly as a result of Arctic amplification associated with global warming and sea ice loss (reviewed by *Barnes and Screen* [2015], *Coumou et al*. [2015], *Screen and Simmonds* [2014], *Horton et al*. [2015], and many others) or change in the tropical climate [e.g., *Yoon et al*., 2014]. A great variety of hypotheses have been proposed regarding anthropogenic induced circulation change and consequent changes in extremes, but as is true for many aspects of the atmosphere's dynamical response to greenhouse gas forcings [*Palmer*, 2013; *Shepherd*, 2014; *Xie et al*., 2015], our understanding is currently inadequate for definitively substantiating or refuting them.

2. Objective, Experiment, and Analysis

The general goal of this study is to quantify to what extent summertime subseasonal variability of surface air temperature (TAS) is enhanced by the end of the 21st century in a 30-member climate change projection from Community Earth System Model version1 (CESM1-LE [*Kay et al*., 2015]) and to diagnose the reasons for any enhancement. We focus on the Great Plains because it has experienced a number of major heat waves/droughts in history [*Namias*, 1982, *Schubert et al*., 2004] and because, as we will show below, this region exhibits the most pronounced enhancement of summertime TAS variability in response to greenhouse gas forcing in CESM1-LE.

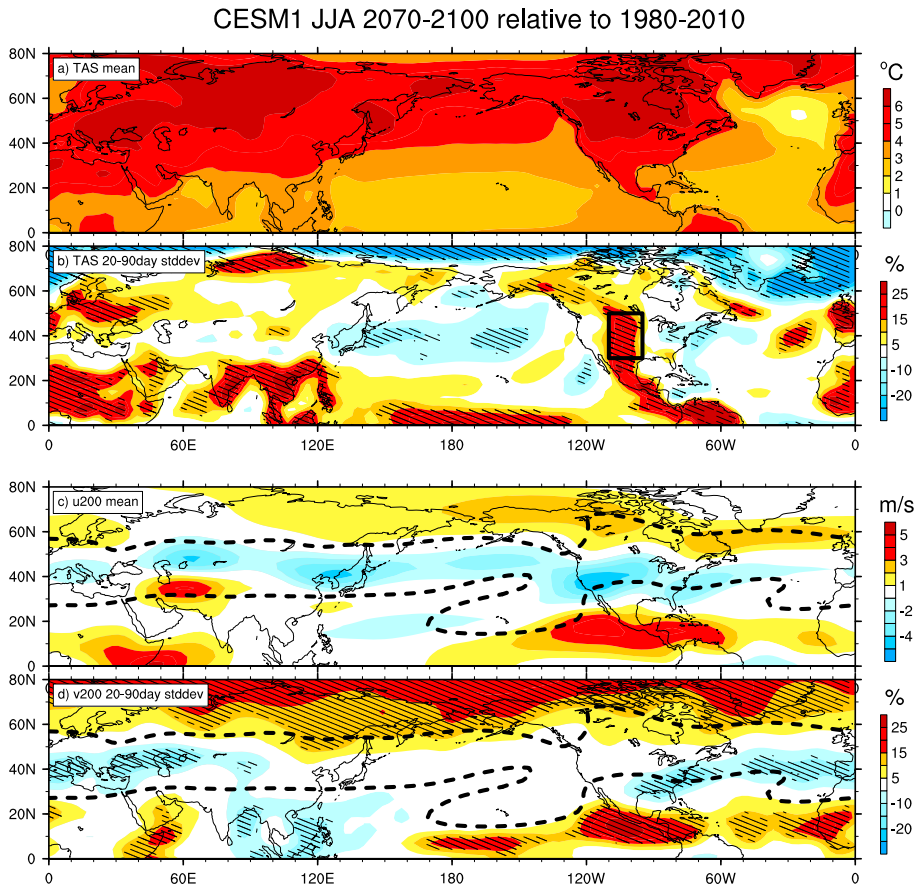

Figure 1. Change in JJA seasonal mean and subseasonal variability from 1980–2010 to 2070–2100 in CESM1-LE. (a and c) Seasonal mean change in surface air temperature (TAS) and 200 hPa zonal wind (u200) respectively. (b and d) Percentage change in standard deviation of 20–90 day filtered TAS and 200 hPa meridional wind (v200). Thick dashed lines in Figures 1c and 1d denote the 10 m/s contour of seasonal mean u200, and hatching indicates the 95% significance level for the variability change from an *F* test. The domain for the Great Plains in this study is outlined by the black line in Figure 1b.

The experiment is forced with historical forcing from 1920 to 2005 and with the Representative Concentration Pathway 8.5 scenario during 2006–2100. Our analysis is mainly focused on June–August (JJA) for the two epochs 1980–2010 and 2070–2100, which represent the present climate and the future climate under a high greenhouse gas emission scenario, respectively. For each epoch, the climatology of a given day during a particular year is calculated as the 30 day running average of the 30-member ensemble mean for that day. Throughout the study, daily anomalies at each grid point are defined as departures from these time-evolving climatologies. Because the response to external forcing is embedded in the time-evolving climatologies, the daily anomalies represent only internal variability of the climate system. We then apply a 20–90 day Lanczos filter [*Duchon*, 1979] to the daily anomalies to separate subseasonal anomalies from high-frequency synoptic eddies.

3. Results

The climatological mean JJA TAS change for 2070–2100 relative to 1980–2010 is about 5–6°C in the Northern Hemisphere midlatitudes (Figure 1a), with the land having stronger warming than the ocean and the amplitude of the warming generally increasing with latitude. Based on the percentage change in the standard deviation of 20–90 day TAS anomalies (Figure 1b), the TAS subseasonal variability is increased by about 20% in 2070–2100 over a number of regions, including Europe, the north coast of Russia, tropical areas in Africa and Asia, and the U.S. Great Plains. There is also reduced temperature variability over some ocean areas. Such variability change is insensitive to the frequency band of the temporal filter that we employed, as

switching to a 2–8 day band yields a similar change regarding both spatial pattern and magnitude. However, there is a strong seasonal dependence in the change in TAS variability. For both the 20–90 day subseasonal anomalies and 2–8 day synoptic eddies, JJA is the only season that exhibits enhanced TAS variability over several continental areas in the Northern Hemisphere midlatitudes; in other seasons the change in TAS variability is either negative or insignificant.

To the extent that temperature anomalies are well approximated by a Gaussian distribution, increases in TAS variability are associated with enhanced amplitudes of extremes. When we find the 97.5th percentile threshold for each calendar day's daily unfiltered anomalies as described above and then calculate the JJA average of these thresholds in each epoch, the change in the threshold values (Figure S1a) yields a similar spatial pattern to the change in TAS variability (Figure 1b). At regions with enhanced temperature variability, such as Europe, the north coast of Russia, and the Great Plains, there is about a 1°C increase in the warm tail of TAS anomalies.

The change in the temperature variability in the Great Plains is further illustrated by comparing probability distribution functions (PDF) of daily TAS anomalies within 110°W–95°W, 30°–50°N (domain outlined in Figure 1b) in JJA from the two epochs (Figure S2). In this figure, the PDFs are based on the aggregate of anomalies on each day of JJA and at each grid point within the region. The standard deviation increases from a value of 2.5°C to a value of 2.9°C. The broadening of the future PDF is not symmetric. While the 97.5th percentile increases from 5.0°C to 5.9°C, the 2.5th percentile has a smaller decrease from −5.0°C to −5.5°C. Based on a plot that shows future change in skewness and kurtosis in TAS anomalies at each grid point in the Northern Hemisphere (Figures S1b and S1c), we find that the Great Plains is one of the regions with the strongest positive change in skewness and negative change in kurtosis, both supporting there will be more hot extremes at the Great Plains in the future climate. We repeat the above calculation with the daily TAS from National Centers for Environmental Prediction/National Center for Atmospheric Research (NCEP/NCAR) reanalysis [*Kalnay et al.*, 1996] during 1980–2010 (green line in Figure S2). With only one realization from the real world, uncertainty in the resulting estimates of variability and tails is substantial. But the estimates that result, namely, a standard deviation of 2.8°C and a 2.5% warm tail threshold at 5.2°C indicate that CESM1-LE's simulation of present day conditions is reasonable, thus giving us some confidence in using this model to study future change in temperature variability in the Great Plains.

Since regional climate is strongly affected by atmospheric circulation, one wonders whether the enhanced summertime TAS subseasonal variability in CESM1-LE is caused by atmospheric circulation changes. Stronger anthropogenic warming at higher latitudes reduces the mean meridional temperature gradient and therefore weakens the upper tropospheric jet stream by thermal wind balance. In CESM1-LE, there is an almost zonally uniform 2 m/s reduction in the JJA mean jet (Figure 1c), and a similar feature was found in other CMIP5 climate change projections [*Simpson et al.*, 2014].

Motivated by the tight connections between regional extremes and quasi-stationary planetary waves found in many studies [*Schubert et al.*, 2011; *Screen and Simmonds*, 2014; *Wang et al.*, 2010; *Teng et al.*, 2013], next we quantify quasi-stationary planetary wave variability by considering the standard deviation of 20–90 day 200 hPa meridional wind (v200) anomalies. We focus on 200 hPa because the upper troposphere is where planetary waves are most pronounced. Wind anomalies in the lower troposphere, e.g., at 850 hPa (v850), may have a stronger influence on surface conditions, including extreme events, than v200 anomalies have. But if we study variability in the circulation at such a low level, it will be more complex and difficult to interpret since both planetary wave dynamical processes and interactions with the surface will be involved.

Unlike the more zonally uniform reduction in the JJA mean jet (Figure 1c), changes in v200 subseasonal variability (Figure 1d) are not uniform. There is a roughly 10% reduction in the region along the jet from the Atlantic Ocean to the Middle East. The intensity of synoptic eddies represented by 2–8 day v200 is reduced by about 15% in this same region (Figure S3), likely as a result of the mean state being less baroclinically unstable. The consistent reduction in both synoptic and subseasonal varability is consistent with the symbiotic relationship between synoptic and quasi-stationary planetary waves that many investigations have pointed out [*Cai and Mak*, 1990; *Branstator*, 1992, 1995; *Schubert et al.*, 2011].

Several studies proposed that the future climate may intensify regional extremes by resonant amplification of planetary waves with certain scales, namely, zonal wave numbers 6–8 [*Petoukhov et al.*, 2013; *Coumou et al.*, 2014]. To test whether this mechanism may play a role in the CESM1-LE experiment, even though in general planetary wave variability has decreased to the east of the Great Plains (Figure 1d), we carry out an analysis similar to that used in previous studies [*Petoukhov et al.*, 2013; *Coumou et al.*, 2014]. We decompose the 20–90 day JJA

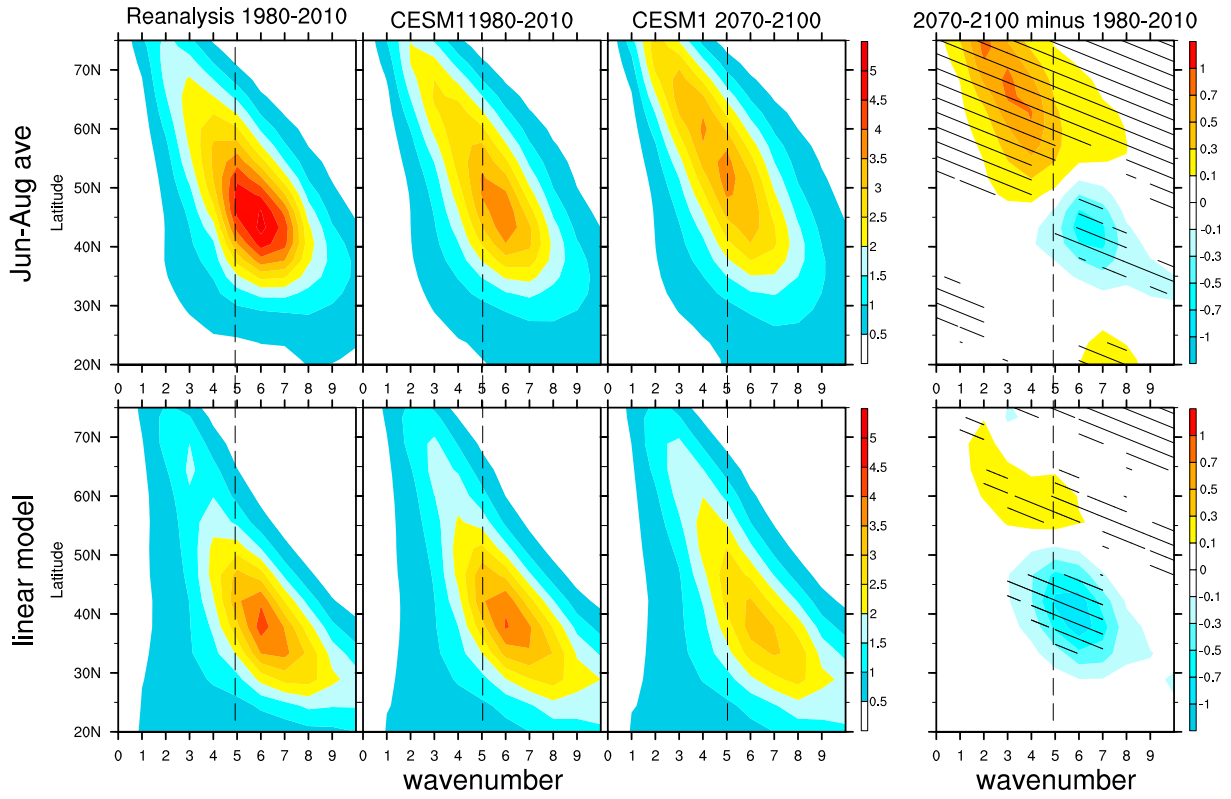

Figure 2. (top row) Zonal wave variance of 20–90 day-filtered JJA 200 hPa meridional wind (v200) anomalies averaged in the Reanalysis during (first column) 1980–2010(left), in (second and third columns) CESM1-LE during 1980-2010 and 2070-2100, and (fourth column) the difference in the two epochs. (Bottom row) same as the top row but from the linear stationary wave model forced with mean states in Figure 2 (top row). Hatching indicating the 95% significance level from Student's *t* test.

v200 anomalies into different Fourier zonal wave numbers at each latitude and use the variance of individual components (Figure 2, top row) as our second metric of planetary wave variability. For the present day, CESM1-LE successfully simulates the variance maximum associated with wave numbers 5 and 6 at 40°–50°N in NCEP-NCAR reanalysis fields, despite other biases including weak wave variance in the midlatitudes and strong variance farther north (top left two panels in Figure 3). The trapped energy along the mean jet is a reflection of the jet acting as a waveguide for disturbances of this scale [*Branstator*, 1983; *Hoskins and Ambrizzi*, 1993; *Branstator*, 2002]. For the future climate, contrary to the resonant amplification of planetary wave hypothesis raised by *Petoukhov et al.* [2013] and *Coumou et al.* [2014], there is less planetary wave energy trapped in the waveguide at 30°–50°N, despite enhanced wave variance north of 50°N.

That the change in the planetary wave variability in CESM1-LE can be attributed to the structure of the change in the mean state can be tested with a simplified dynamical framework. We employ the same model described in *Branstator* [1990] except that (a) 10 equally spaced vertical levels are used, (b) the horizontal truncation is R15, and (c) the damping coefficients are set to $(2\,\text{days})^{-1}$ at all vertical levels. We set the basic state in a stationary planetary wave model that is based on the linearized primitive equations to the JJA mean air temperature, wind, and surface pressure from each of the two epochs in CESM1-LE. For each basic state, we force the model with random global distributions of steady vorticity sources that are intended to represent the scattering of energy among modes normally produced by nonlinear processes. When 1000 such solutions are analyzed in the same way that the CESM1-LE solutions are analyzed to produce plots of the zonal wave variance of v200, the similarity of the results to those for CESM1-LE (Figure 2, bottom row) confirms that the future reduced wave variance in the midlatitudes and enhanced variance at high latitudes in CESM1-LE is caused by changes in the mean climate.

Our third metric for planetary wave variability is keyed on heat waves in the Great Plains. We devote our attention to events during which at least 20% of the grid points in the Great Plains have at least five consecutive days during which the averaged TAS anomaly exceeds a threshold value. This threshold corresponds

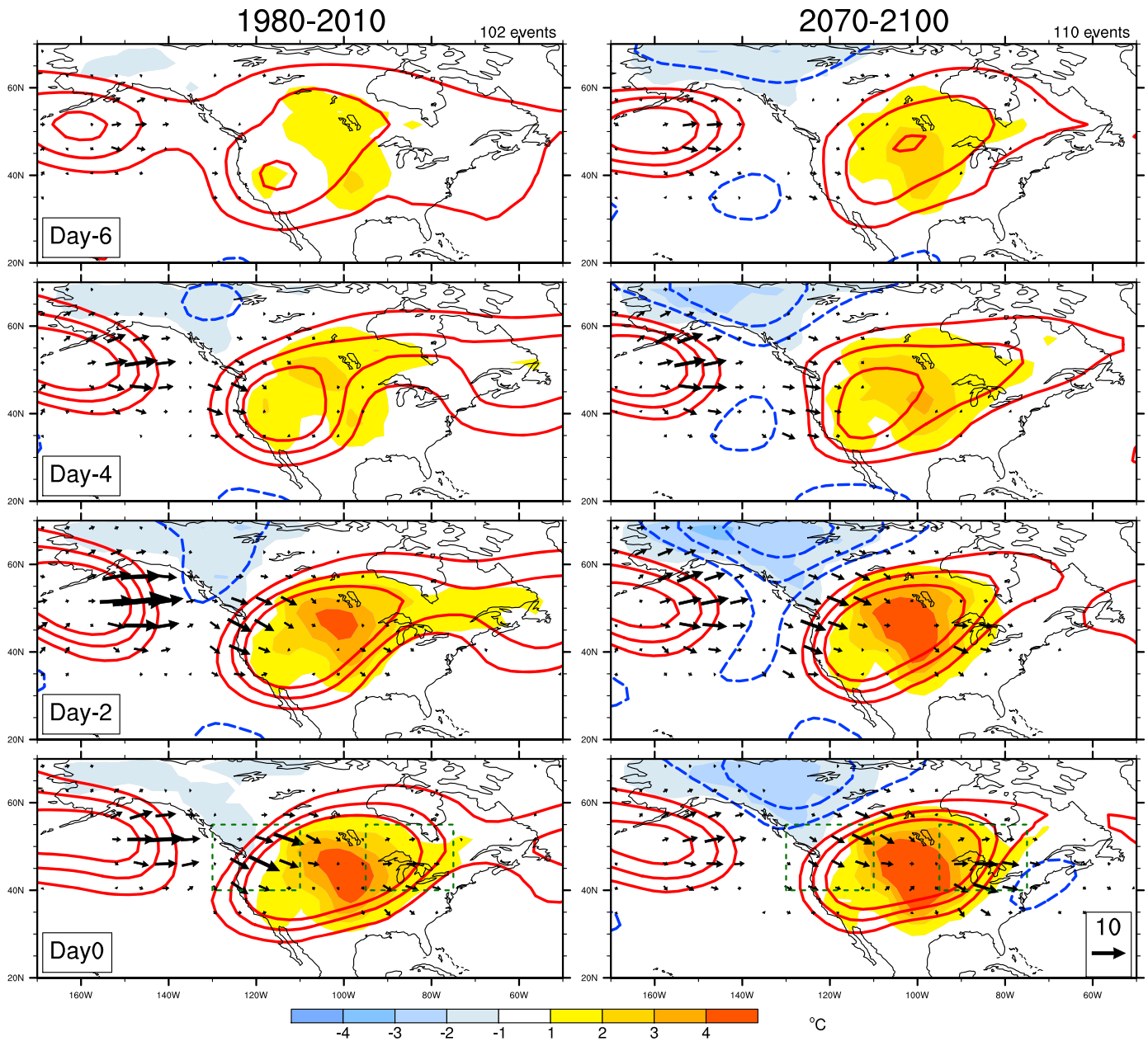

Figure 3. Composite of daily anomalies of 200 hPa streamfunction (contour), surface air temperature (shading), and Plumb flux (vector [*Karoly et al.*, 1989]) from 102 present-day and 110 future heat waves in the Great Plains. For clarity only contour levels of the stream function anomalies at $\pm 1,2,3 \times 10^6 m^2 s^{-1}$ are displayed, and Plumb flux vectors with magnitude less than 1 $m^2 s^{-2}$ are not shown.

to the 97.5th percentile of an epoch's climatological distribution within a 30 day running window centered on a particular day of the year. (Note each distribution is based on $30 \times 30 \times 31$ daily anomalies, so that nearly 700 days surpass the threshold.) In addition, we only use cases for which there are no heat waves in the preceding 15 days. With the combined criteria, we find 102 and 110 events from the present and future epoch, respectively.

For both epochs, the U.S. continent is dominated by a quasi-stationary anticyclonic circulation anomaly (Figure 3) from day-6 to day0, where day0 is the first day that a persistent heat wave exists. This anticyclone is part of a zonal wave number-5 Rossby wave pattern trapped in the midlatitude jet stream waveguide [*Hoskins and Karoly*, 1981; *Branstator*, 1983; *Hoskins and Ambrizzi*, 1993; *Teng et al.*, 2013]. A second

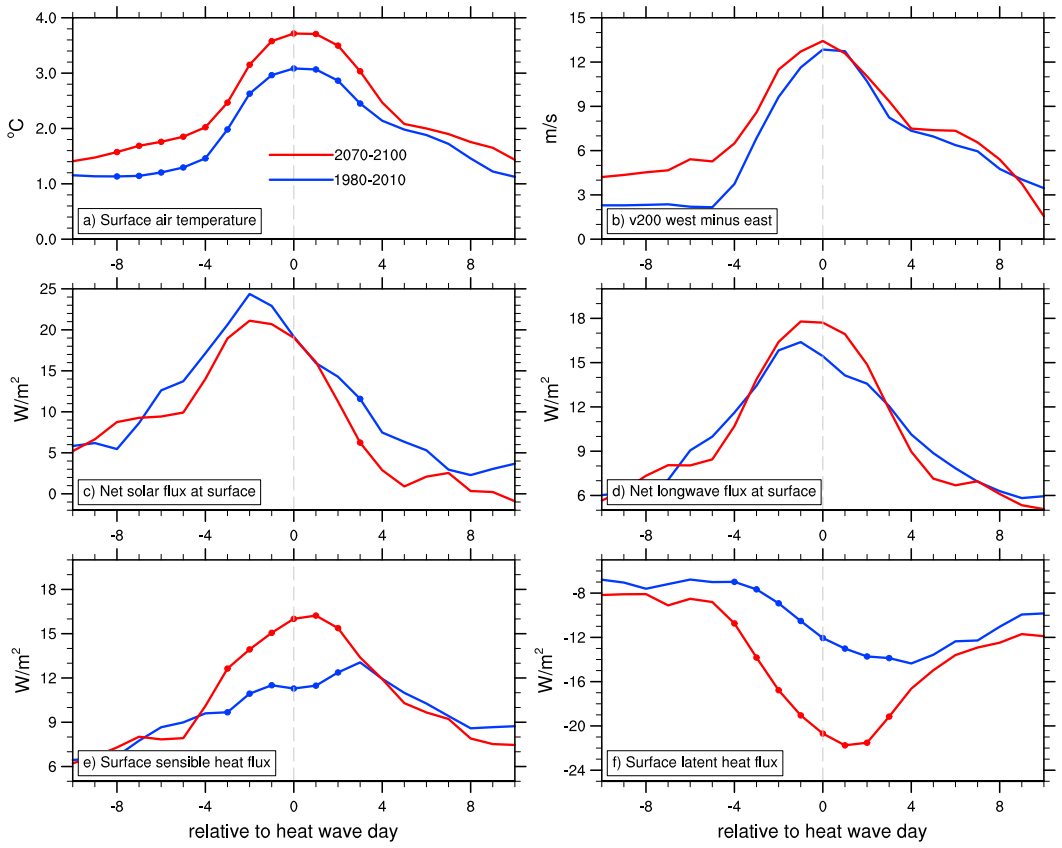

Figure 4. Surface energy balance for the Great Plain heat waves. Domain averaged anomalies of (a) surface air temperature, (b) upper troposphere anticyclone strength, (c) net shortwave, (d) longwave radiation, (e) sensible, and (f) latent heat flux at surface from day−10 to day10 of the heat waves in the two epochs. Strength of the anticyclone as measured by the difference between 200 hPa meridional wind (v200) anomalies at 40°–55°N, 130°–110°W, and 40°–50°N, 95°–75°W (outlined in Figure 3, bottom row), while the other five variables are averaged within 110°W–95°W, 30°–50°N. Blue and red lines represent heat wave composite anomalies during 1980–2010 and 2070–2100, respectively. Dots denote that the composite values are significantly different at the 95% level between 1980–2010 and 2070–2100.

anticyclone is located upstream over the north Pacific, and, as represented by the Plumb flux, [*Plumb*, 1985; *Karoly et al*., 1989, equation (1)] wave energy propagates downstream from the North Pacific toward the U.S. for at least a week before the heat waves occur. In addition to Rossby wave dispersion, momentum fluxes from synoptic eddies are involved in the generation of this pattern [*Teng et al*., 2013].

The TAS anomalies in Figure 3 indicate that heat waves are stronger in the future model climate, and the amplification is quantified by averaging TAS anomalies over the Great Plains (Figure 4a). The anticyclone aloft is measured by the difference in v200 averaged in two boxes, one to the west (40°–55°N, 130°–110°W) and one to the east (40°–55°N, 95°–75°W) of the Great Plains (outlined in Figure 3, bottom row). Even though the TAS anomalies associated with the future heat waves are on average 0.6°C warmer than the present-day values, the anticyclone anomalies aloft exhibit no significant change in the two epochs (Figure 4b), just as planetary wave subseasonal variability, in general, has not changed in that region (Figure 1d). The most pronounced change in the upper level circulation is the deepened cyclone over Alaska and northern Canada in the future climate (Figure 3), which is consistent with enhanced planetary wave variance at higher latitudes in the future climate (Figure 2, fourth column). However, this strengthening appears to be too far north to contribute to the warmer heat waves. We have also made a similar plot for 850 hPa streamfunction anomalies, where the circulation can have a more direct influence on surface temperature, and again, we do not find significant circulation change at latitudes where heat waves occur (Figure S4).

In contrast to our results for planetary waves, the local surface energy balance provides a plausible cause for the amplified future heat waves. Although neither the net shortwave nor the net longwave radiation

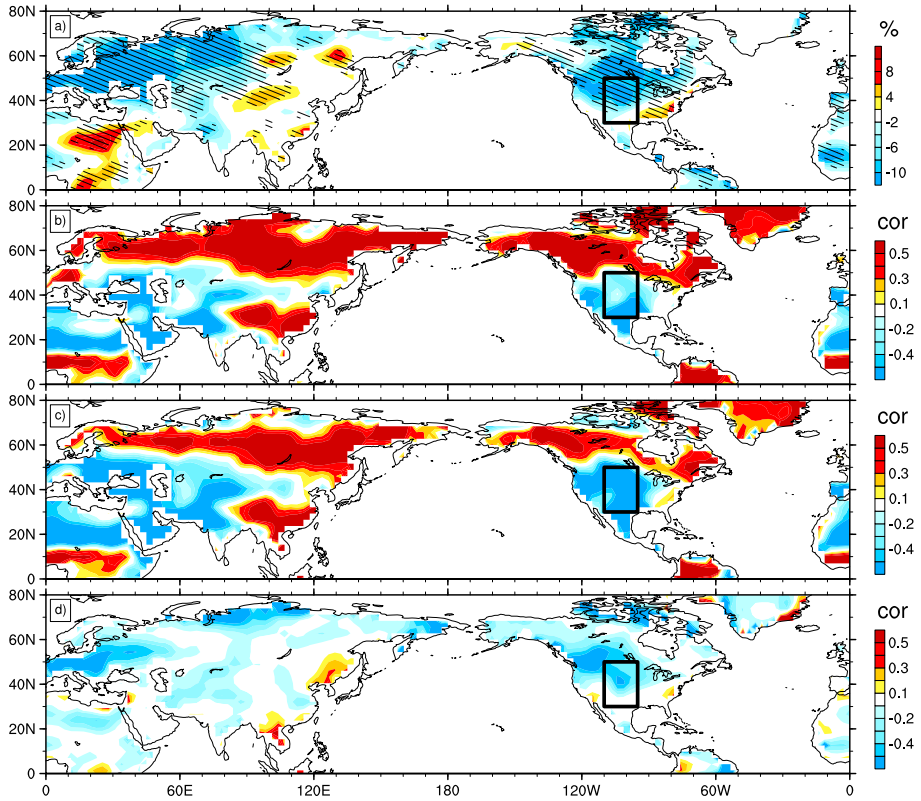

Figure 5. Percentage change in (a) JJA-averaged upper 10 cm soil water and correlation coefficients between JJA subseasonal monthly TAS and evaportranspiration anomalies in (b) 1980–2100, (c) 2070–2100, and (d) their difference in Figure 5c minus Figure 5b. The 99% significance level for correlation coefficients with 2790 degree of freedom (30 member × 31 years × 3 months) is approximately 0.05.

anomalies exhibit significant changes before the heat waves in reaction to the changing climate (Figures 4c and 4d), in the future climate there are significantly increased surface sensible heat flux anomalies compensated by reduced latent heat anomalies before and during the heat waves (Figures 4e and 4f).

Increased Bowen ratio is expected in the future summers as the mean soil moisture is significantly reduced (Figure 5a). Furthermore, the Great Plains is one of the regions where TAS variability is strongly coupled to soil moisture [*Koster et al.*, 2004; *Seneviratne et al.*, 2006, 2010; *Diffenbaugh and Ashfaq*, 2010; *Wang et al.*, 2015]. Following *Seneviratne et al.* [2006, 2010], we use correlation coefficient between subseasonal TAS and evaportranspiration anomalies (Figures 5b and 5c) to diagnose TAS-soil moisture coupling. While positive correlations in Figures 5bc denote lack of such coupling [*Seneviratne et al.*, 2010], negative correlations, e.g., those in the Great Plains (Figures 5b and 5c), indicate drier soil can reduce evapotranspiration, which leads to an increase in sensible heat flux and thus an increase in TAS. Greater TAS may potentially further decrease soil moisture, leading to a positive feedback between soil moisture and TAS [*Seneviratne et al.*, 2010].

We find in CESM1-LE as the mean soil moisture is reduced in the future climate (Figure 5a), the coupling strength measured by the absolute value of the correlation coefficients further increases at the northern Great Plains (Figure 5d). This location coincides with where TAS anomalies exhibit the most pronounced growth in the 95th percentile (Figure S1a). It is also the region where the TAS anomalies during the future heat waves are most amplified (Figure 3). Therefore, even without amplified planetary waves in the future climate in CESM1-LE, subseasonal TAS variability can be enhanced due to reduction in the mean soil moisture and enhanced TAS-soil moisture coupling.

4. Conclusion

Based on a 30-member climate change projection from an earth system model, we find that summertime subseasonal temperature variability in the U.S. Great Plains is enhanced by about 20% in 2070–2100 relative

to 1980–2010. Furthermore, daily temperature departures from the new mean during future heat waves are on average about 0.6°C warmer than are the corresponding departures under present-day conditions. The amplified temperature variability and heat waves in the Great Plains appear to be primarily caused by enhanced local land-atmosphere coupling resulting from a warmer/drier future climate.

Despite numerous hypotheses (reviewed by *Barnes and Screen* [2015]) by which anthropogenic climate change might intensify future midlatitude extremes by enhancing planetary wave variability, such mechanisms, which in earlier studies were either based on a simple model or the relatively short observational records, do not appear to make significant contributions to the strengthening of summertime subseasonal temperature variability and heat waves in the Great Plains in CESM1-LE. Thus, our results provide a good example of how extreme events can be affected by climate change through processes that do not involve amplified planetary wave variability.

Acknowledgments

CESM1-LE output was postprocessed by Gary Strand and is available from the Earth System Grid (http://www.earthsystemgrid.org). This study was supported by the Regional and Global Climate Modeling Program (RGCM) of the U.S. Department of Energy's, Office of Science (BER), Cooperative Agreement DE-FC02-97ER62402 and by the National Energy Research Scientific Computing Center, which is supported by Office of Science of the U.S. Department of Energy under contract DE-AC02-05CH11231 and by the National Science Foundation. G.B. acknowledges supports by NOAA MAPP NA14OAR4310224 and NASA NEWS via NA09OAR4310187. The National Center for Atmospheric Research is sponsored by the National Science Foundation.

References

Barnes, E. A., and J. A. Screen (2015), The impact of Arctic warming on the midlatitude jetstream: Can it? Has it? Will it?, *WIREs Clim. Change*, *6*, 277–286.

Branstator, G. (1983), Horizontal energy propagation in a barotropic atmosphere with meridional and zonal structure, *J. Atmos. Sci.*, *40*, 1689–1708.

Branstator, G. (1990), Low-frequency patterns induced by stationary waves, *J. Atmos. Sci.*, *47*, 629–648.

Branstator, G. (1992), The maintenance of low-frequency atmospheric anomalies, *J. Atmos. Sci.*, *49*, 1924–1946.

Branstator, G. (1995), Organization of storm track anomalies by recurring low-frequency circulation anomalies, *J. Atmos. Sci.*, *52*, 207–226.

Branstator, G. (2002), Circumglobal teleconnections, the jet stream waveguide, and the North Atlantic Oscillation, *J. Clim.*, *15*, 1893–1910.

Cai, M., and M. Mak (1990), Symbiotic relation between planetary and synoptic-scale waves, *J. Atmos. Sci.*, *47*, 2953–2968.

Cattiaux, J., H. Douville, R. Schoetter, S. Parey, and P. Yiou (2015), Projected increase in diurnal and interdiurnal variations of European summer temperatures, *Geophys. Res. Lett.*, *42*, 899–907, doi:10.1002/2014GL062531.

Coumou, D., V. Petoukhov, S. Rahmstorf, S. Petri, and H. J. Schellnhuber (2014), Quasi-resonant circulation regimes and hemispheric synchronization of extreme weather in boreal summer, *Proc. Natl. Acad. Sci. U.S.A.*, *111*, 12,331–12,336.

Coumou, D., J. Lehmann, and J. Beckmann (2015), The weakening summer circulation in the Northern Hemisphere mid-latitude, *Science*, *348*, 324–327.

Diffenbaugh, N. S., and M. Ashfaq (2010), Intensification of hot extremes in the United States, *Geophys. Res. Lett.*, *37*, L15701, doi:10.1029/2010GL043888.

Duchon, C. E. (1979), Lanczos filtering in one and two dimensions, *J. Appl. Meteorol.*, *18*, 1016–1022.

Fischer, E. M., S. I. Seneviratne, P. L. Vidale, D. Lüthi, and C. Schär (2007), Soil moisture-atmosphere interaction during the 2003 European summer heat wave, *J. Clim.*, *20*, 5081–5099.

Fischer, E. M., D. M. Lawrence, and B. M. Sanderson (2011), Quantifying uncertainties in projections of extremes: A perturbed land surface parameter experiment, *Clim. Dyn.*, *37*, 1381–1398, doi:10.1007/s00382-010-0915-y.

Fischer, E. M., J. Rajczak, and C. Schär (2012), Changes in European summer temperature variability revisited, *Geophys. Res. Lett.*, *39*, K19702, doi:10.1029/2012GL052730.

Gregory, J. M., and J. F. B. Mitchell (1995), Simulation of daily variability of surface-temperature and precipitation over Europe in the current and 2×CO_2 climates using the UKMO climate model, *Q. J. R. Meteorol. Soc.*, *121*, 1451–1476.

Horton, D. E., N. C. Johnson, D. Singh, D. L. Swain, B. Rajaratnam, and N. S. Diffenbaugh (2015), Contribution of changes in atmospheric circulation patterns to extreme temperature trends, *Nature*, *522*, 465–469.

Hoskins, B. J., and T. Ambrizzi (1993), Rossby wave propagation on a realistic longitudinally varying flow, *J. Atmos. Sci.*, *50*, 1661–1671.

Hoskins, B. J., and D. J. Karoly (1981), The steady linear response of a spherical atmosphere to thermal and orographic forcing, *J. Atmos. Sci.*, *38*, 1179–1196.

Kalnay, E., et al. (1996), The NCEP/NCAR 40-year reanalysis project, *Bull. Am. Meteorol. Soc.*, *77*, 437–471.

Karoly, D. J., R. A. Plumb, and M. Ting (1989), Example of the horizontal propagation of quasi-stationary waves, *J. Atmos. Sci.*, *46*, 2802–2811.

Katz, R. W., and B. G. Brown (1992), Extreme events in a changing climate: Variability is more important than averages, *Clim. Change*, *21*, 289–302.

Kay, J. E., et al. (2015), The Community Earth System Model (CESM) large ensemble project: A community resource for studying climate change in the presence of internal climate variability, *Bull. Am. Meteorol. Soc.*, doi:10.1175/BAMS-D-13-00255.1.

Kim, O.-Y., B. Wang, and S.-H. Shin (2013), How do weather characteristics change in a warming climate?, *Clim. Dyn.*, *41*, 3261–3281, doi:10.1007/s00382-013-1795-8.

Kjellström, E., L. Bärring, D. Jacob, R. Jones, G. Lenderink, and C. Schär (2007), Modelling daily temperature extremes: Recent climate and future changes over Europe, *Clim. Change*, *81*(Suppl 1), 249–265, doi:10.1007/s10584-006-9220-5.

Koster, R. D., et al. (2004), Regions of strong coupling between soil moisture and precipitation, *Science*, *305*, 1138–1140.

Meehl, G. A., and C. Tebaldi (2004), More intense, more frequent, and longer lasting heat waves in the 21st century, *Science*, *305*, 994–997.

Namias, J. (1982), Anatomy of Great Plains protracted heat waves (especially the 1980 U.S. summer drought), *Mon. Weather Rev.*, *110*, 824–838.

Palmer, T. N. (2013), Climate extremes and the role of dynamics, *Proc. Natl. Acad. Sci. U.S.A.*, *110*, 5281–5282.

Petoukhov, V., S. Rahmstorf, S. Petri, and H. J. Schellnhuber (2013), Quasiresonant amplification of planetary waves and recent Northern Hemisphere weather extremes, *Proc. Natl. Acad. Sci. U.S.A.*, *110*, 5336–5341.

Plumb, R. A. (1985), On the three-dimensional propagation of stationary waves, *J. Atmos. Sci.*, *42*, 217–229.

Schär, C., P. L. Vidale, D. Lüthi, C. Frei, C. Häberli, M. A. Liniger, and C. Appenzeller (2004), The role of increasing temperature variability in European summer heatwaves, *Nature*, *427*, 332–336.

Schneider, T., T. Bischoff, and H. Plotka (2014), Physics of changes in synoptic midlatitude temperature variability, *J. Clim.*, doi:10.1175/JCL-D-14-00632.1.

Schubert, S., M. J. Suarez, P. J. Pegion, R. D. Koster, and J. T. Bacmeister (2004), Causes of long-term drought in the U.S. Great Plains, *J. Clim.*, *17*, 485–503.
Schubert, S., H. Wang, and M. Suarez (2011), Warm seasonal subseasonal variability and climate extremes in the Northern Hemisphere: The role of stationary Rossby waves, *J. Clim.*, doi:10.1175/JCLI-D-10-05035.1.
Screen, J. A. (2014), Arctic amplification decreases temperature variance in northern mid- to high-latitudes, *Nat. Clim. Change*, *4*, 577–582.
Screen, J. A., and I. Simmonds (2014), Amplified mid-latitude planetary wave favor particular regional weather extremes, *Nat. Clim. Change*, *4*, 704–709.
Screen, J. A., C. Deser, and L. Sun (2015), Reduced risk of North America cold extremes due to continued Arctic sea ice loss, *Bull. Am. Meteorol. Soc.*, doi:10.1175/BAMS-D-14-00185.
Seneviratne, S. I., D. Lüthi, M. Litschi, and C. Schär (2006), Land–atmosphere coupling and climate change in Europe, *Nature*, *443*, 205–209.
Seneviratne, S. I., T. Corti, E. L. Davin, M. Hirschi, E. B. Jaeger, I. Lehner, B. Orlowsky, and A. J. Teuling (2010), Investigating soil moisture-climate interactions in a chaging climate: A review, *Earth Sci. Rev.*, *99*, 125–161.
Shepherd, T. G. (2014), Atmospheric circulation as a source of uncertainty in climate change projections, *Nat. Geosci.*, *7*, 703–708.
Simpson, I., T. A. Shaw, and R. Seager (2014), A diagnosis of the seasonally and longitudinally varying midlatitude circulation response to global warming, *J. Atmos. Sci.*, *71*, 2489–2515.
Taylor, K. E., R. J. Stouffer, and G. A. Meehl (2012), An overview of CMIP5 and the experiment design, *Bull. Am. Meteorol. Soc.*, *93*, 485–498.
Teng, H., G. Branstator, H. Wang, G. A. Meehl, and W. M. Washington (2013), Probability of US heat waves affected by a subseasonal planetary wave pattern, *Nat. Geosci.*, *6*, 1056–1061.
Wang, S.-Y., L. E. Hipps, R. R. Gillies, X. Jiang, and A. L. Moller (2010), Circumglobal teleconnection and early summer rainfall in the U.S. Intermountain West, *Theor. Appl. Climatol.*, *102*, 245–252.
Wang, S.-Y., et al. (2015), An intensified seasonal transition in the Central U.S. that enhances summer drought, *J. Geophy. Res. Atmos.*, *120*, 8804–8816, doi:10.1002/2014JD023013.
Xie, S.-P., et al. (2015), Towards predictive understanding of regional climate change, *Nat. Clim. Change*, *5*, 921–930.
Yoon, J.-H., S.-Y. S. Wang, R. R. Gillies, B. Kravitz, L. Hipps, and P. J. Rasch (2014), Increasing water cycle extremes in California and in relation to ENSO cycle under global warming, *Nat. Commun.*, doi:10.1038/ncomms9657.